Supplementary Information

Fabrication and *in situ* functionalisation of mesoporous silica films by the physical entrapment of functional and responsive block copolymer structuring agents†

Jessica C. Tom,[a] C. Appel[b], Annette Andrieu-Brunsen*[a]

[a]Ernst-Berl Institut für Technische und Makromolekulare Chemie, Technische Universität Darmstadt, Alarich-Weiss-Straße 12, 64287 Darmstadt, Germany
[b]Institute of Condensed Matter Physics, Technische Universität Darmstadt, Hochschulstraße 8, 64289 Darmstadt, Germany
*Corresponding author: andrieu-brunsen@smartmem.tu-darmstadt.de.

Table of Contents

Materials

All materials and solvents were purchased from Sigma-Aldrich and used as received unless stated otherwise. The monomers used, styrene (S, 99 %) and *tert*-butyl acrylate (*t*BA, Alfa Aesar, 99 %), were passed over a small column of either basic or neutral alumina to remove the inhibitor immediately prior to use. *N*,*N*′,*N*′′,*N*′′-Pentamethyldiethylenetriamine (PMDETA, 99 %), tris[2-(dimethylamino)ethyl]amine (Me_6TREN, Alfa Aesar, 97 %), ethyl α-bromoisobutyrate (EBiB, 98 %), and copper(II) bromide ($CuBr_2$, 98 %) were used without further purification. The copper(0) wire catalyst (Aldrich, >99.9 %, 1 mm diameter) used in all polymerisations was activated using hydrochloric acid (37 %) for 8 min before being rinsed thoroughly with acetone, and drying under a nitrogen stream before being stored under vacuum until use. The solvents used for polymerisation, dichloromethane (DCM, Carl Roth, Rotisol, ≥ 99.8 %) and *N*,*N*-dimethylformamide (DMF, anhydrous, 99.8 %) were used as received. The side chains bearing *tert*-butyl ester groups were hydrolysed to acrylic acid units using trifluoroacetic acid (TFA, Carl Roth, ≥99.9 %).

The precursor solutions for dip-coating were prepared using the inorganic precursor tetraethoxysilane (TEOS, Acros Organics, 98 %) alone or in combination with an organosilane such as (3-aminopropyl)trimethoxysilane (APTMS, Acros Organics 95 %) in either dry tetrahydrofuran (THF, Merck, SeccoSolv) or absolute ethanol (EtOH, Merck, ≥99.5 %), with a hydrochloric acid catalyst (HCl, 37 %) and Milli-Q water. The template used was either synthesised PS-*b*-PAA with varying molecular weights or Pluronic® F-127 (F127, BioReagent, 13,800 g mol^{-1}). The microscope slides (VWR, glass, cut edges) were cleaned with detergent and milli-Q water prior to rinsing with ethanol and allowing to air dry. The silicon wafers (Si-Mat, 100 mm diameter, 525 ± 25 µm thickness, type P/Bor, <100> orientation, CZ growth method, 2–5 Ω resistivity, polished on 1 side, Kaufering, Germany) and indium tin oxide (ITO, Delta Technologies, Ltd., polished float glass, 150 × 150 × 1.1 mm^3, SiO_2 passivated / Indium Tin Oxide coating on one surface, RS = 4–8 Ω, cut edges) were cut to an appropriate size using a diamond cutter, cleaned using technical-grade ethanol, and air-dried prior to dip-coating in a Binder GmbH climate chamber (Model KBF 240).

Analytical Methods

^1H NMR Spectroscopy

^1H NMR spectra were recorded on a 300 MHz Bruker AVANCE NMR spectrometer (Billerica, MA, USA) in deuterated chloroform ($CDCl_3$, 99.8 % D), DMSO (DMSO-d_6, 99.9 % D), or methanol (MeOD, 99.8 % D). The solvent residual peak was used as an internal reference.

Size Exclusion Chromatography (SEC)

SEC (Agilent Scientific Instruments, Santa Clara, CA, USA) was performed using a PSS-Agilent 1200 instrument equipped with a 1200 Agilent RID, a 1050 UV detector, and an autosampler (100 µL). The filtered samples were passed through a SDV 5 µm pre-column (8 × 50 mm) and a PSS SDV LIN M 5 µm column (8 × 300 mm) using tetrahydrofuran (THF) as eluent at a flow rate of 1 mL min^{-1} at 40 °C. The molecular weight and molecular weight distribution was determined using WinGPC UniChrom software (Version 8.20 build 4815, PSS Polymer Standards Service GmbH, Mainz, Germay, 1992–2014) by conventional calibration with linear polystyrene standards ranging between 3.75×10^{-3} and 3.23×10^{-6} g mol^{-1} with toluene as a flow rate marker.

Attenuated Total Reflectance Fourier Transform Infrared Spectroscopy (ATR-FTIR)

A Perkin Elmer Instruments One Spectrum FT-IR Spectrometer equipped with a Universal ATR Polarization Accessory (Waltham, MA, USA) was used to characterise the mesoporous films prepared on either glass or ITO substrates. All spectra result from averaging at least 3 spots taken directly from the film surface at a resolution of 4 cm^{-1}, and are normalised to the Si-O-Si band at ~1085 cm^{-1}. All spectra were recorded from 4000 to 650 cm^{-1} and background corrected automatically by the Spectrum Software (Version 10.5.4.738, PerkinElmer, Inc., Waltham, USA, 2016). All further data corrections were carried out in OriginPro9 (ADDITIVE Soft- und Hardware für Technik und Wissenschaft GmbH, Friedrichsdorf, Germany, 2012).

Macroscopic Static Contact Angle (CA)

Static contact angle (CA) measurements were performed on a DataPhysics OCA35 instrument (DataPhysics Instruments GmbH, Filderstadt, Germany) using SCA20 software (Version 4.5.15 build 1064, DataPhysics Instruments GmbH, Filderstadt, Germany, 1998–2013) and the sessile drop method. The CA was measured within 30 s of applying a 2 µL water droplet onto the surface at a rate of 2 µL s^{-1}. All CA measurements were conducted within a climate-controlled room at 25 °C and 50 % humidity. All CAs are averaged from at least five measurements taken across the film surface, and are reported with a standard deviation as error.

Ellipsometry

Mesoporous films were prepared on silicon wafer substrates to determine the average film thickness and refractive index using a Nanofilm EP3 imaging ellipsometer equipped with a 658 nm laser. Each film was characterised at 3 spots along the surface, and measurements were recorded at a fixed humidity of 15 % and ambient temperature varying the angle of incidence (AOI) from 38 to 66 ° in one zone. The film thickness and refractive index was then determined using the EP4 analysis software supplied with the instrument from the measured amplitude and phase difference, Ψ and Δ, respectively.

A one-layer box model was used to fit the data assuming a 2.2 nm oxide layer is present between the silicon wafer substrate and mesoporous film based on previous measurements and fitting. One-layer films were allowed to vary between 10 and 300 nm, with a refractive index between 1 and 1.7. Two-layer systems were allowed to vary between 10 and 600 nm. The volume porosity was then calculated from the fitted refractive index according to the Brüggemann effective medium approximation.[1, 2]

Cyclic Voltammetry (CV)

The electrochemical and transport behaviour of these mesoporous materials under filled and unfilled conditions was investigated via cyclic voltammetry (CV) using $[Fe(CN)_6]^{4-/3-}$ and $[Ru(NH_3)_6]^{2+/3+}$ as negative and positive probe molecules, respectively. Mesoporous films prepared on ITO substrates were characterised using a Metrohm Autolab PGSTAT302N potentiostat (Metrohm, Utrecht, Netherlands) with a 1 mM solution of either the positive or negative probe molecule in a 100 mM KCl electrolyte solution. The pH-dependent permselectivity was investigated by adjusting the solution pH between 2 and 11 by the addition of either aqueous NaOH or HCl to the prepared solutions. The pH was determined using pH-Fix 0–14 indicator sticks (Laborbedarf, Article No. 0549, Carl Roth, Karlsruhe, Germany). A Ag/AgCl reference electrode (BASi RE-6) and graphite counter electrode was used in the sample cell. The electrode area was 0.21 cm^2; however, all measurements reported here correspond to the peak currents in µA. Each pH was measured using a scan rate sequence of 200, 100, 25, 300, 1000, and 200 mV s^{-1}, with each scan rate cycled three times. All voltammograms shown here correspond to the last cycle measured at a scan rate of 100 mV s^{-1}, and bare ITO was measured as a reference on each measurement day for comparison.

Ultraviolet–Visible Spectroscopy (UV-Vis)

UV-Vis spectra were recorded using an Agilent Technologies Cary 60 UV-Vis spectrophotometer equipped with a full spectrum Xenon pulse lamp single source. The spectra were background corrected using the corresponding solvent. Each spectrum was recorded between 800 and 300 nm at a scan speed of 600 nm min^{-1}. A square aperture quartz cell with a 1.0 cm path length was used for all measurements.

Dynamic Light Scattering (DLS)

DLS was performed on a Malvern Zetasizer Nano-ZS at a fixed scattering angle of 90 ° with a He–Ne Laser (633 nm) at 25 °C to determine the size and shape of the micelles formed by the prepared block copolymers in aqueous solutions. A 1.0 mg mL^{-1} dispersion was prepared by first dissolving the block copolymer in THF before adding the appropriate amount of Milli-Q water and removing the THF under reduced pressure at 40 °C. The dispersions were then diluted and filtered through a PVDF filter prior to measurements. The mean diameter or Z-average size of the micelles was determined from 3 measurements resulting from 12 consecutive runs, each 60 s in duration. For all measurements, a plastic disposable cuvette with a 1.0 cm path length was used.

Scanning Electron Microscopy (SEM)

SEM spectra were obtained using a Philips XL30 FEG scanning electron microscope equipped with a tungsten cathode and a back scattered electron yttrium aluminium garnet (BSE YAG) detector at an accelerating voltage of 15–25 kV, a 30 µm aperture, and a spot size of 4–5. The samples were sputter-coated with a 5 nm coating of Pt/Pd. The digital micrographs were recorded at a working distance of ~10 nm with an SE2 detector.

Transmission Electron Microscopy (TEM)

Electron micrographs were recorded using a Philips FEI CM-20 transmission electron microscope (Philips, Amsterdam, The Netherlands) equipped with a LAB-6 cathode and Olympus CCD camera, and with a maximum resolution of 2.3 Å operating at an accelerating voltage of 200 kV. Samples were prepared by scratching the mesoporous films off the substrate and dispersing in filtered ethanol with 10 min of sonication before being drop cast onto 3.05 mm Cu grids (mesh size 200) with a Lacey carbon film (Plano GmbH, article number S166-2). The samples were then dried under ambient conditions.

Grazing Incidence Small-Angle X-ray Scattering (GISAXS)

GISAXS data was recorded using a Rigaku SmartLab X-ray diffractometer with a GiSAXS option. The K_α-line of a copper X-ray tube with a wave length of $\lambda = 0.154$ nm is used and further monochromated by an X-ray mirror. The point-focused beam is collimated by three pinholes. The scattered intensity is measured with a semiconductor pixel detector HyPix-3000 with 775x385 px^2 and a pixel size of 100 µm. The sample-detector distance is 300 mm resulting in an instrumental resolution of $\Delta q_{||} = 0.04$ nm^{-1}. The scattering vectors are defined as $q_{||} = (q_x^2 + q_y^2)^{0.5} = 2\pi/\lambda\ ((\cos(\alpha_f)\cos(\chi) - \cos(\alpha_i))^2 + (\cos(\alpha_i)\sin(\chi))^2)^{0.5}$ and $q_z = 2\pi/\lambda\ ((\sin(\alpha_i) + \sin(\alpha_f))$ with α_i and α_f respectively the in-plane incident and exit angles in direction of the beam, and χ the out of plane angle.

Experimental Procedures

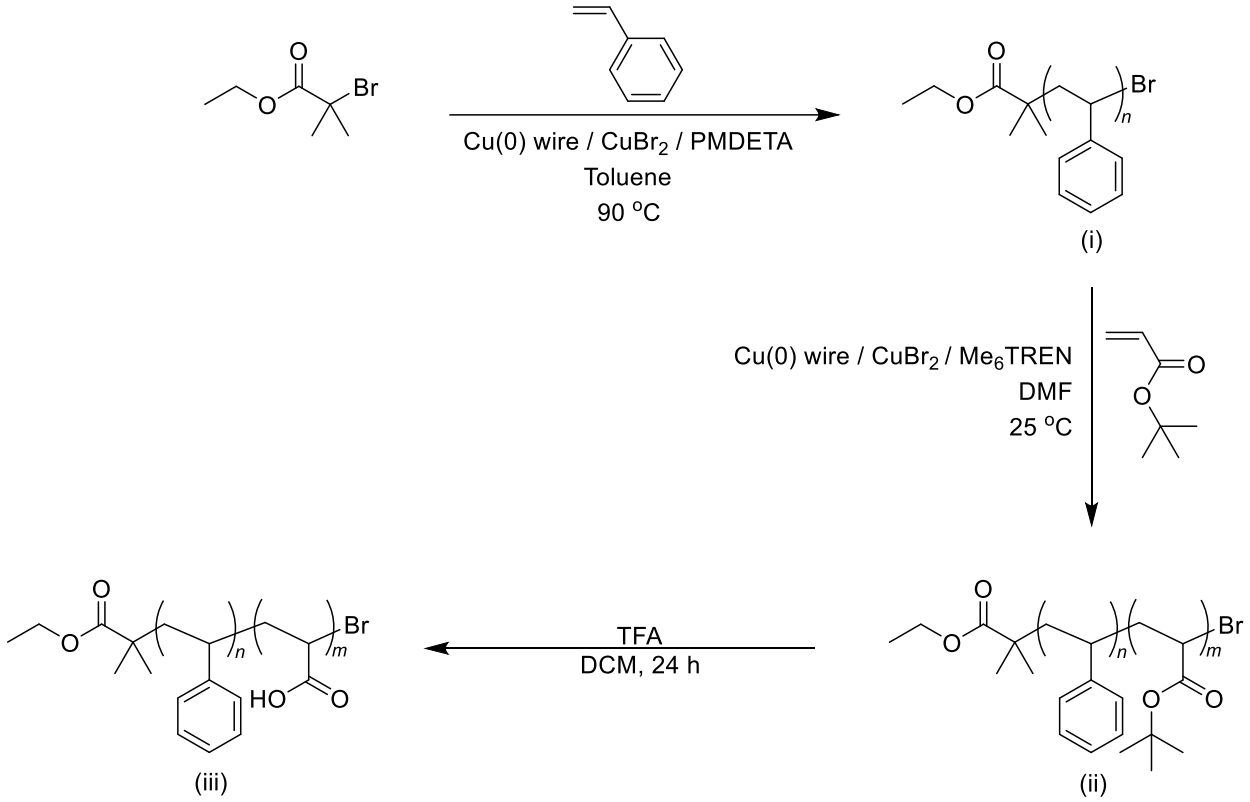

Scheme S1 Synthetic pathway used to prepare functional amphiphilic block copolymers of PS-*b*-PAA to both structure and functionalise mesoporous silica.

Synthesis of linear polystyrene, $DP_{n,target}$ 25, via SET-LRP[3]

Copper(II) bromide (29.0 mg, 1.30×10^{-1} mmol) and PMDETA (95.4 µL, 4.57×10^{-1} mmol) were dissolved in toluene (3.0 mL). To this mixture, styrene (6.0 mL, 52 mmol) and initiator (EBiB, 191.5 µL, 1.305 mmol) were added. The reaction mixture was then transferred to a Schlenk tube charged with a copper(0) wire catalyst (1 mm diameter, 2 cm length, HCl-activated) wrapped around a magnetic stirrer bar, which was maintained above the solution using an external magnet. The reaction mixture was then deoxygenated by 3 consecutive freeze-pump-thaw cycles before being back-filled with nitrogen. The flask was then placed into a thermostatted oil bath preheated to 90 ºC before the external magnet was removed to release the copper(0) wire catalyst into solution to initiate the polymerisation. The polymerisation was quenched by cooling and exposure to air after 24 h. The dissolved copper complex was removed by first diluting the polystyrene macroinitiator with THF and passing it over a column of neutral alumina before precipitation into a 10-fold excess of ice-cold methanol. The polystyrene was collected by vacuum filtration to yield a white powder. SEC (THF, 1 mL min^{-1}, 40 °C): $M_{n,SEC}$ = 4200 g mol^{-1}, $M_{w,SEC}$ = 4565 g mol^{-1}, $Đ$ = 1.09. $\%C_{NMR}$ = 96.0 %, $M_{n,th}$ = 4150 g mol^{-1}. $DP_{n,th}$ = 38. ATR (cm^{-1}, 4 cm^{-1}): 3026, 2922, 2850, 1726, 1602, 1493, 1452, 1028, 907, 756, 697.

Preparation of PS_{38}-*b*-P*t*BA_{46} via SET-LRP

A polystyrene macroinitiator ($M_{n,th}$ = 4150 g mol^{-1}, $DP_{n,th}$ = 38, 1.15 g, 2.77×10^{-1} mmol) bearing an alkyl halide end-group was first dissolved in DMF (1.81 mL). Then, a DMF stock solution (200 µL) containing $CuBr_2$ (3.1 mg, 1.40×10^{-2} mmol) and Me_6TREN (13.3 µL, 5.0×10^{-2} mmol) was added to the dissolved macroinitiator before the monomer *tert*-butyl acrylate (2.01 mL, 13.9 mmol) was added. The reaction mixture was then transferred to a Schlenk tube charged with a copper(0) wire catalyst (1 mm diameter, 3 cm length, HCl-activated) wrapped around a magnetic stirrer bar, which was maintained above the solution using an external magnet. The reaction vessel was then sealed with a rubber septum before being deoxygenated by purging with nitrogen in an ice bath for 10 min. The solution was then allowed to equilibrate in a 25 °C water bath before the catalyst was released into solution to initiate the polymerisation. The polymerisation was quenched by exposure to air after 4 h. The mixture was diluted with THF and passed over a column of neutral alumina to remove the dissolved copper. The resulting block copolymer was obtained by removing the residual monomer and solvent under reduced pressure. SEC (THF, 1 mL min^{-1}, 40 °C): $M_{n,SEC}$ = 12780 g mol^{-1}, $M_{w,SEC}$ = 13740 g mol^{-1}, $Đ$ = 1.08. $\%C_{NMR}$ = 91 %, $M_{n,th}$ (block) = 5896 g mol^{-1}. $DP_{n,th}$ (block) = 46. ATR (cm^{-1}, 4 cm^{-1}): 2977, 2926, 1724, 1602, 1493, 1480, 1452, 1392, 1367, 1255, 1144, 1030, 845, 750, 697.

Preparation of PS_{38}-*b*-PAA_{46} by hydrolysis of PS_{38}-*b*-P*t*BA_{46}

A 10-fold molar excess with respect to the *tert*-butyl ester groups of trifluoroacetic acid (TFA, 10 mL, 131 mmol) was added to a solution of PS_{38}-*b*-$PtBA_{46}$ (2.9 g, mmol 13.3 mmol tert-butyl ester) in DCM (20 mL). The reaction mixture was then stirred under ambient conditions for 24 h before being concentrated under reduced pressure at 40 ºC. The white solid was then redissolved in THF before being precipitated in a 10-fold excess of cold hexane. The white solid was collected by vacuum filtration and dried in a vacuum oven at 40 °C for 2 days. The successful hydrolysis to acrylic acid was confirmed by the disappearance of the *tert*-butyl ester band observed at ~1370 cm^{-1} by ATR and ^1H NMR. ATR (cm^{-1}, 4 cm^{-1}): 3025, 2921, 2564, 1703, 1493, 1451, 1417, 1242, 1160, 1112, 1060, 1027, 804, 755, 697.

Preparation of PS_{38}-*b*-P*t*BA_{100} via SET-LRP

A polystyrene macroinitiator ($M_{n,th}$ = 4150 g mol^{-1}, $DP_{n,th}$ = 38, 1.2 g, 2.89 × 10^{-1} mmol) bearing an alkyl halide end-group was first dissolved in DMF (4 mL). Then, a DMF stock solution (200 µL) containing $CuBr_2$ (3.26 mg, 1.46 × 10^{-2} mmol) and Me_6TREN (13.9 µL, 5.2 × 10^{-2} mmol) was added to the dissolved macroinitiator before the monomer *tert*-butyl acrylate (4.2 mL, 28.9 mmol) was added. The reaction mixture was then transferred to a Schlenk tube charged with a copper(0) wire catalyst (1 mm diameter, 6 cm length, HCl-activated) wrapped around a magnetic stirrer bar, which was maintained above the solution using an external magnet. The reaction vessel was then sealed with a rubber septum before being deoxygenated by purging with nitrogen in an ice bath for 20 min. The solution was then allowed to equilibrate in a 25 °C water bath before the catalyst was released into solution to initiate the polymerisation. The polymerisation was quenched by exposure to air after 17 h. The mixture was diluted with THF and passed over a column of neutral alumina to remove the dissolved copper. The resulting block copolymer was obtained by removing the residual monomer and solvent under reduced pressure, and the tert-butyl ester groups were then hydrolysed using TFA without any further purification. SEC (THF, 1 mL min^{-1}, 40 °C): $M_{n,SEC}$ = 20,950 g mol^{-1}, $M_{w,SEC}$ = 23,510 g mol^{-1}, $Đ$ = 1.12. $\%C_{NMR}$ = 100 %, $M_{n,th}$ (block) = 12,820 g mol^{-1}. $DP_{n,th}$ (block) = 100. ATR (cm^{-1}, 4 cm^{-1}): 2977, 2931, 1724, 1684, 1601, 1494, 1480, 1453, 1392, 1367, 1253, 1143, 1031, 845, 752, 698.

Preparation of PS_{38}-*b*-PAA_{100} by hydrolysis of PS_{38}-*b*-P*t*BA_{100}

A 10-fold molar excess with respect to the *tert*-butyl ester groups of trifluoroacetic acid (TFA, 10 mL, 131 mmol) was added to a solution of PS_{38}-*b*-P*t*BA_{100} (2.45 g, mmol 14.4 mmol *tert*-butyl ester) in DCM (20 mL). The reaction mixture was then stirred under ambient conditions for 24 h before being concentrated under reduced pressure at 40 ºC. The white solid was then redissolved in THF before being precipitated in a 10-fold excess of cold hexane. The white solid was collected by vacuum filtration and dried in a vacuum oven at 40 °C for 2 days. The successful hydrolysis to acrylic acid was confirmed by the disappearance of the *tert*-butyl ester band observed at ~1370 cm^{-1} and ^1H NMR. ATR (cm^{-1}, 4 cm^{-1}): 2923, 2559, 1699, 1494, 1450, 1417, 1242, 1163, 1107, 1062, 1026, 802, 756, 697.

Synthesis of linear polystyrene, $DP_{n,target}$ 50, via SET-LRP[3]

Copper(II) bromide (13.6 mg, 6.09 × 10^{-2} mmol) and PMDETA (44.9 µL, 2.15 × 10^{-1} mmol) were dissolved in toluene (3.0 mL). To this mixture, styrene (6.0 mL, 52 mmol) and initiator (EBiB, 90.1 µL, 6.14 × 10^{-1} mmol) were added. The reaction mixture was then transferred to a Schlenk tube charged with a copper(0) wire catalyst (1 mm diameter, 2 cm length, HCl-activated) wrapped around a magnetic stirrer bar, which was maintained above the solution using an external magnet. The reaction mixture was then deoxygenated by 3 consecutive freeze-pump-thaw cycles before being back-filled with nitrogen. The flask was then placed into a thermostatted oil bath preheated to 90 °C before the external magnet was removed to release the copper(0) wire catalyst into solution to initiate the polymerisation. The polymerisation was quenched by cooling and exposure to air after 24 h. The dissolved copper complex was removed by first diluting the polystyrene macroinitiator with THF and passing it over a column of neutral alumina before precipitation into a 10-fold excess of ice-cold methanol. The polystyrene was collected by vacuum filtration to yield a white powder. SEC (THF, 1 mL min^{-1}, 40 °C): $M_{n,SEC}$ = 6050 g mol^{-1}, $M_{w,SEC}$ = 6600 g mol^{-1}, $Đ$ = 1.09. $\%C_{NMR}$ = 71.2 %, $M_{n,th}$ = 6444 g mol^{-1}. $DP_{n,th}$ = 60. ATR (cm^{-1}, 4 cm^{-1}): 3025, 2922, 1601, 1493, 1452, 756, 696.

Preparation of PS_{60}-*b*-P*t*BA_{100} via SET-LRP

A polystyrene macroinitiator ($M_{n,th}$ = 6444 g mol^{-1}, $DP_{n,th}$ = 60, 1.0 g, 1.6 × 10^{-1} mmol) bearing an alkyl halide end-group was first dissolved in DMF (2.1 mL). Then, a DMF stock solution (108 µL) containing $CuBr_2$ (1.76 mg, 8.0 × 10^{-3} mmol) and Me_6TREN (7.5 µL, 2.8 × 10^{-2} mmol) was added to the dissolved macroinitiator before the monomer *tert*-butyl acrylate (2.25 mL, 15.5 mmol) was added. The reaction mixture was then transferred to a Schlenk tube charged with a copper(0) wire catalyst (1 mm diameter, 3 cm length, HCl-activated) wrapped around a magnetic stirrer bar, which was maintained above the solution using an external magnet. The reaction vessel was then sealed with a rubber septum before being deoxygenated by purging with nitrogen in an ice bath for 10 min. The solution was then allowed to equilibrate in a 25 °C water bath before the catalyst was released into solution to initiate the polymerisation. The polymerisation was quenched by exposure to air after 4 h. The mixture was diluted with THF and passed over a column of neutral alumina to remove the dissolved copper. The resulting block copolymer was obtained by removing the residual monomer and solvent under reduced pressure, and the *tert*-butyl ester groups were then hydrolysed using TFA without any further purification. SEC (THF, 1 mL min^{-1}, 40 °C): $M_{n,SEC}$ = 15450 g mol^{-1}, $M_{w,SEC}$ = 18850 g mol^{-1}, $Đ$ = 1.22. $\%C_{NMR}$ = 84 %, $M_{n,th}$ (block) = 10770 g mol^{-1}. $DP_{n,th}$ (block) = 84. ATR (cm^{-1}): 3026, 2978, 2928, 1724, 1601, 1493, 1480, 1452, 1392, 1366, 1255, 1143, 1029, 908, 845, 750, 697.

Preparation of PS_{60}-*b*-PAA_{84} by hydrolysis of PS_{60}-*b*-P*t*BA_{84}

A 10-fold molar excess with respect to the *tert*-butyl ester groups of trifluoroacetic acid (TFA, 10 mL, 131 mmol) was added to a solution of PS_{60}-*b*-P*t*BA_{84} (3.01 g, mmol 14.7 mmol *tert*-butyl ester) in DCM (20 mL). The reaction mixture was then stirred under ambient conditions for 24 h before being concentrated under reduced pressure at 40 °C. The white solid was then redissolved in THF before being precipitated in a 10-fold excess of cold hexane. The white solid was collected by vacuum filtration and dried in a vacuum oven at 40 °C for 2 days. The successful hydrolysis to acrylic acid was confirmed by the disappearance of the *tert*-butyl ester band observed at ~1370 cm^{-1} and ^1H NMR. ATR (cm^{-1}, 4 cm^{-1}): 3029, 2921, 2565, 1703, 1493, 1451, 1416, 1243, 1157, 1108, 1060, 1027, 906, 802, 754, 696.

Preparation of mesoporous silica using the prepared block copolymer templates

The precursor solutions used for dip-coating were prepared using a mixture of tetraethoxysilane (TEOS) and a functional block copolymer structuring agent (PS-*b*-PAA) dissolved in THF in the presence of an aqueous acid catalyst. The TEOS:BCP:THF:H_2O:HCl molar ratio used was fixed at 1:0.0075:40:10.8:0.28 for all block copolymers examined. The solutions were left under ambient conditions with vigorous stirring for 24 h before being frozen to prevent further hydrolysis before use.

The precursor solutions were then used to prepare mesoporous silica single and double layer films through dip-coating on glass, silicon wafer, and ITO substrates at a relative humidity of 50 % and a temperature of 25 °C at a withdrawal speed of 2 mm s^{-1}. After allowing the films to dry in a climate-controlled room (1 h, 25 °C, 50 % r.H.), the films were subjected to a stabilising thermal treatment. This involved 2 successive treatments at 60 and 120 °C for 1 h each, before the temperature was increased at a rate of 1 °C min^{-1} to 200 °C, which was maintained for a period of 2 h before the films were allowed to cool to room temperature.

Supplementary Results

Structural Characterisation of the Synthesised Block Copolymer Templates

Size exclusion chromatography (SEC) clearly shows that the prepared polystyrene macroinitiators have been successfully chain-extended with *tert*-butyl acrylate in a controlled manner (Figure S1). A small quantity of PS macroinitiator remains due to the loss of the active chain end with a low molecular weight shoulder observed in good agreement with the PS macroinitiator.

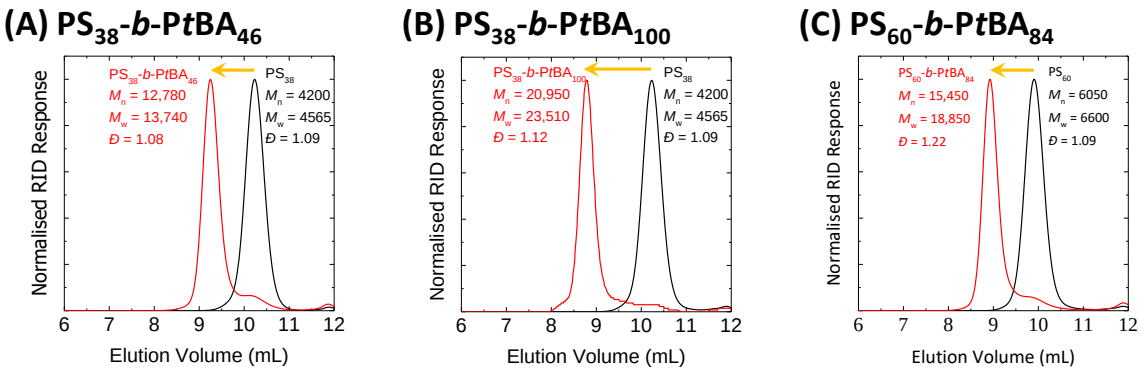

Figure S1 SEC traces of the PS macroinitiator before (black curve) and after (red curve) chain extension with tBA to prepare (A) PS_{38}-*b*-$PtBA_{46}$, (B) PS_{38}-*b*-PAA_{100}, and (C) PS_{60}-*b*-PAA_{84}.

After hydrolysis of the *tert*-butyl acrylate block to acrylic acid, their thermal stability in air was examined by thermal gravimetric analysis (TGA). Figure S2 shows the degradation profiles and corresponding derivative weight loss curves of each respective block copolymer prepared. After the evaporation of water (<150 °C), the block copolymers appear relatively stable, undergoing only a slight degradation at a temperature of 180–205 °C before exhibiting a major thermal decomposition between 320 and 450 °C. Therefore, we are confident that the functional moieties of the prepared structuring agents largely survive the harsh calcination conditions of 200 °C for 2 h, further supported by IR spectroscopy (Figure 3).

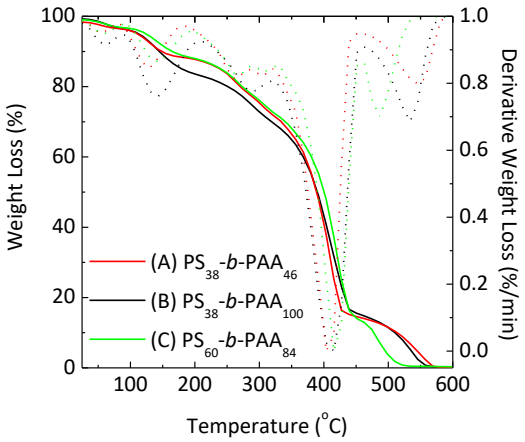

Figure S2 Thermal gravimetric analysis and corresponding derivative weight loss of (A) PS_{38}-*b*-PAA_{46} (red trace), (B) PS_{38}-*b*-PAA_{100} (black trace), and (C) PS_{60}-*b*-PAA_{84} (green trace). The samples were heated from 25 to 600 °C at a rate of 10 °C min^{-1} under an air flow of 30 mL min^{-1}.

Self-Assembly Behaviour

The ability of such polymers to self-assemble under typical dip-coating conditions and concentrations was first assessed prior to applying them in a sol for EISA. PS_{38}-*b*-PAA_{100} was first dissolved in THF, and the increase in turbidity measured by UV-Vis spectroscopy with the progressive addition of water (Figure S3). At a block copolymer concentration of 1.75 wt%, micellar structures are formed at a critical water concentration (cwc) of ~22 wt% in agreement with previously reported data of similar BCPs.[4] Typical formulations used to prepare mesoporous silica in ethanol contain an initial Pluronic® F127 concentration of ~4 wt%, and a water content of 7.5 wt%. Being tolerant to relatively large water concentrations in THF, the prepared block copolymers were deemed suitable for use in EISA.

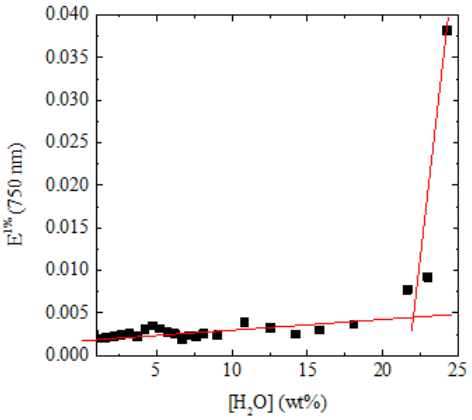

Figure S3 Extinction coefficient (1 % w/v) at 750 nm for a PS_{38}-*b*-PAA_{100} solution in THF with an increasing water content from 0 to 25 wt%. UV-Vis spectra were recorded between 800 and 300 nm at a scan speed of 600 nm min^{-1}.

The structure of the block copolymer assemblies formed in water by each amphiphilic block copolymer was then probed through dynamic light scattering (DLS) with increasing concentration (Figure S4, Table S1). The amphiphilic block copolymers were assembled by dissolution in tetrahydrofuran (THF) followed by the addition of deionised water and removal of the good solvent under reduced pressure.

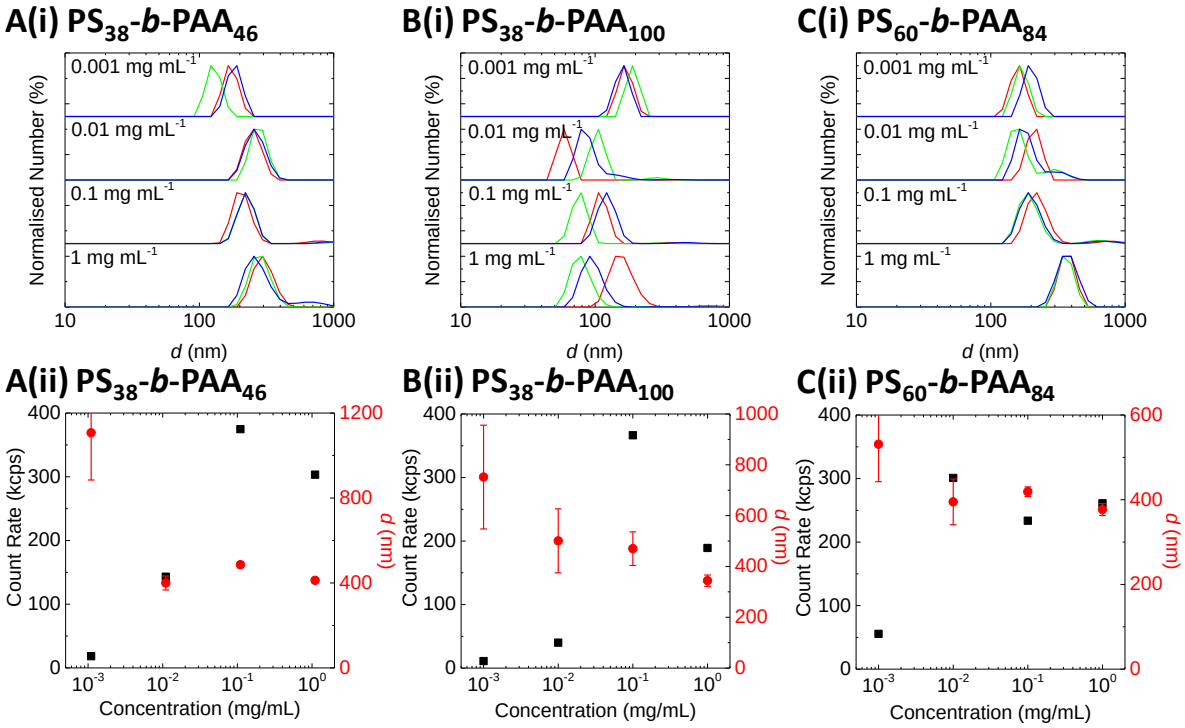

Figure S4 (i) Dynamic light scattering traces, and the corresponding (ii) count rate and hydrodynamic diameter at varying concentrations from 0.001, 0.01, 0.1, and 1 mg mL^{-1} of the block copolymers assembled in water: (A) PS_{38}-*b*-PAA_{46}, (B) PS_{38}-*b*-PAA_{100}, and (C) PS_{60}-*b*-PAA_{84}.

Mathematically, we cannot expect spherical micelles of the prepared block copolymers to exceed 42–73 nm with fully extended polymer chains. As the measured particle size diverges significantly from this maximum size, varying between 344 and 1107 nm depending on the polymer and concentration, it is more likely they form more complex structures such as cylindrical micelles and/or aggregates under the preparation conditions used here, and which are not comparable to those formed *via* the EISA process. Furthermore, the variation in size measured at the same concentration observed in Figure S4 (i) further supports the formation of non-spherical assemblies.

Table S1 Z-average particle size and corresponding dispersity (in parentheses) of the prepared amphiphilic block copolymers in Milli-Q water at 1, 0.1, 0.01 and 0.001 mg mL^{-1}. The standard deviation arising from 3 measurements is reported as error.

Entry	BCP template	Z-ave (nm) at a given concentration (polydispersity index)			
		1 mg mL^{-1}	0.1 mg mL^{-1}	0.01 mg mL^{-1}	0.001 mg mL^{-1}
A	PS_{38}-*b*-PAA_{46}	412.5 ± 12.5 (0.270)	486.0 ± 14.5 (0.642)	399.8 ± 32.8 (0.495)	1106.7 ± 222.3 (0.994)
B	PS_{38}-*b*-PAA_{100}	344.1 ± 22.4 (0.532)	470.1 ± 66.1 (0.652)	500.7 ± 125.9 (0.738)	751.7 ± 204.1 (0.930)
C	PS_{60}-*b*-PAA_{84}	376.7 ± 14.1 (0.063)	419.0 ± 11.4 (0.508)	395.0 ± 54.0 (0.550)	530.9 ± 88.2 (0.804)

The amphiphilic block copolymers were then tested as potential EISA templates to prepare functional pH-responsive mesoporous silica.

Single Layer Mesoporous Silica with and without a Functional Entrapped Polymer

The set of prepared amphiphilic block copolymers with varying hydrophobic to hydrophilic block lengths were then tested as templating agents using a typical sol formulation (TEOS:BCP:THF:H_2O:HCl = 1:0.0075:40:10.8:0.28). After dip-coating the films onto various substrates, the films were dried for 24 h before being subjected to a thermal stabilising treatment. This involved heating the films to a maximum temperature of 200 °C for 2 h due to the thermal stability of the block copolymers. To probe the nature of the mesoporous framework formed in comparison to typical mesoporous silica materials templated with commercial templates, the BCP was burnt out at a temperature of 350 °C. To remove the functional block copolymers the films were heated in 10 min to a temperature of 60 °C, this temperature was maintained for 1 h before heating the films in 10 min to 130 °C, which was again maintained for 1 h before the films were heated to a final temperature of 350 °C at a rate of 1 °C min^{-1}, which was maintained for 2 h. The films were then allowed to cool to ambient temperature before being rinsed with ethanol and dried under ambient conditions. The ellipsometry results before and after this additional thermal treatment to remove the template are summarised in Table S2. The film shrinkage can be attributed to the matrix retraction / collapse upon the removal of the block copolymer template. Since the molar concentration of the polymers was kept constant in the sol relative to TEOS, it is not unexpected that Film B, which was structured using the highest molecular weight block copolymer according to SEC measurements, PS_{38}-*b*-PAA_{100}, experiences the greatest shrinkage.

Table S2 Raw film thickness, refractive index, and volume porosity of the films prepared using PS-*b*-PAA with varying block lengths as a structuring agent. A TEOS:BCP:THF:H_2O:HCl molar ratio of 1:0.0075:40:10.8:0.28 was used in the sol, and the substrates were dip-coated at a withdrawal speed of 2 mm s^{-1} at 50 % r.H. and 25 °C.

Entry	BCP template	With BCP			Without BCP				*Shrinkage*
		d (nm)[a]	*n*[a]	RMSE	*d* (nm)[a]	*n*[a]	RMSE	V_{pore} (%)[b]	(%)[c]
A	PS_{38}-*b*-PAA_{46}	90.0 ± 0.1	1.476 ± 0.001	0.142	86.7 ± 0.3	1.207 ± 0.001	0.165	53.2	3.7
		97.9 ± 0.1	1.448 ± 0.001	0.172	78.0 ± 0.1	1.211 ± 0.000	0.043	52.4	20
		82.0 ± 0.2	1.472 ± 0.002	0.293	73.4 ± 0.1	1.216 ± 0.000	0.060	51.3	10
B	PS_{38}-*b*-PAA_{100}	136.6 ± 0.2	1.514 ± 0.001	1.279	102.4 ± 0.2	1.222 ± 0.001	0.161	50.0	25
		117.2 ± 0.1	1.504 ± 0.001	0.607	91.8 ± 0.3	1.239 ± 0.001	0.183	46.4	22
		115.5 ± 0.1	1.503 ± 0.001	0.624	90.2 ± 0.1	1.232 ± 0.000	0.093	47.9	22
C	PS_{60}-*b*-PAA_{84}	127.6 ± 0.6	1.509 ± 0.005	4.501	131.9 ± 0.1	1.153 ± 0.000	0.071	64.9	-3.0
		130.9 ± 0.1	1.526 ± 0.001	1.307	121.3 ± 0.1	1.154 ± 0.000	0.046	64.7	7.3
		128.5 ± 0.3	1.529 ± 0.002	3.301	107.0 ± 0.1	1.159 ± 0.000	0.080	63.6	17

[a]The pore diameter, *d*, and the refractive index, *n*, were measured using ellipsometry at a relative humidity of 15 % and at ambient temperature at 3 positions along the film.
[b]The film porosity, V_{pore}, was calculated according to the Brüggemann effective medium approximation from the fitted refractive index.
[c]The film shrinkage upon calcination by heating to 350 °C was calculated as a percentage of the initial film thickness.

Ionic Permselectivity under Filled and Empty Conditions

Cyclic voltammetry (CV) was used to investigate the ionic permselectivity towards both positive and negative charges of the functional mesoporous silica films prepared on ITO substrates before and after removing the entrapped functional block copolymers. The CV traces cycling between extreme pH values is shown in Figure S5.

Removal of the amphiphilic block copolymers affords ionic permselectivity behaviour akin to unfunctionalised mesoporous silica templated by commercial templates like Pluronic® F127 (Figure S5(ii)). This observation further confirms that the prepared amphiphilic block copolymers are retained after consolidating the silica framework at 200 °C for a period of 2 h, and result in the observed enhancement in ionic permselectivity and gating properties observed (Figure 4, Figure S5(i)).

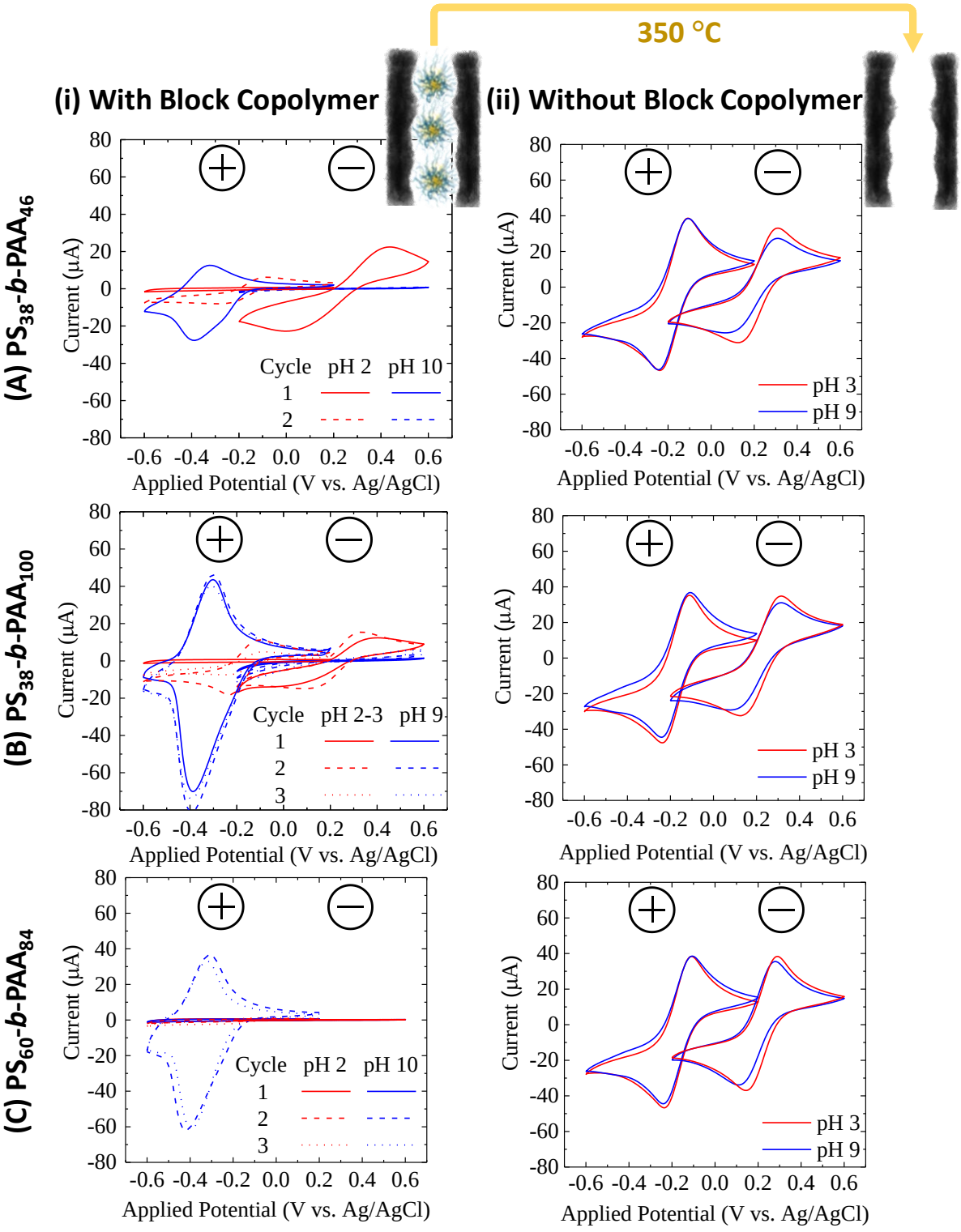

Figure S5 Cyclic voltammograms of the prepared mesoporous silica templated using the synthesised block copolymer templates: (A) PS_{38}-*b*-PAA_{46}, (B) PS_{38}-*b*-PAA_{100}, and (C) PS_{60}-*b*-PAA_{84}, (i) with and (ii) without the functional BCP. The functional block copolymer template was removed by a thermal treatment at 350 °C for comparison. The CV traces were recorded at a scan rate of 100 mV s^{-1} in 100 mM KCl with $Fe(CN)_6^{4-/3-}$ or $Ru(NH_3)_6^{2+/3+}$ at a concentration of 1 mM. The reference ITO CV traces varied between approximately +40 and −40 µA, and have been omitted for simplicity.

The first noteworthy observation is that the films must be cycled once between extreme pH values to activate the films due to wetting. We can attribute this to the reformation of the micelle structure in an aqueous environment. This behaviour further supports the disruption of the micelle structure formed during the calcination step, together with the high contact angles between 75–85 º observed before the template is removed by thermal degradation at 350 ºC (Table 1). PAA has also been shown to adsorb to silica through the formation of hydrogen bridges,[5] and this could render the pore surface hydrophobic due to the PS block masking the hydrophilic pore wall, and further hinder the transport of aqueous solutions. However, with increasing pH, less PAA is adsorbed to the surface due to electrostatic repulsion between the negatively charged pore wall and formed carboxylate ions.[5] Once the micelles are reformed within the pores and the hydrophobic PS block is again buried within the centre of the micelle, the films exhibit ionic permselectivity in an aqueous environment similar to that observed by mesoporous silica prepared using F127 where the pore diameter is less than the Debye screening length.[6]

From the CV traces after burning out the template at 350 °C (Figure S5), it is clear that the pore diameter in these films exceeds the Debye screening length, with both positive and negative charges able to pass through the structure unhindered regardless of the pH when the block copolymer template is not present to control the transport properties. This is consistent with the measured micelle size by DLS of the prepared block copolymer templates (Table 1, Figure S4). Hence, the transport properties displayed by these films arises predominantly from the block copolymer charge and micelle size, which impacts the pore diameter, and hence the proximity of the probe molecules to the pore wall.

Some general trends observed in the ionic permselectivity of films with BCP structure:

- Under basic conditions where the pore wall and acrylic acid moieties are negatively charged, higher peak currents are observed for positively-charged species due to electrostatic attraction, despite the high degree of pore filling.
- Increasing the total number of acrylic acid units within the mesopores leads to enhanced permselectivity of positive charged species.
- Increasing the amount of hydrophobic styrene units leads to the complete exclusion of negatively charged species from entering the porous framework. This may arise from poor shielding of the hydrophobic core by the hydrophilic corona (Film B and Film C), and hence poor wetting preventing the flow of aqueous solutions. Under basic conditions, due to the repulsion between the negatively charged walls and shell, the polymer assemblies likely contract resulting in larger free space and improved wetting.

In addition to these interesting observations, the BCP-containing films exhibit clear preconcentration by adsorption of the positively-charged probe to the negatively-charged pore wall and carboxylate ions under basic conditions, as evidenced by the broadened shape and shift in the oxidation peak to lower potentials.[7] For (B) and (C), where the entrapped block copolymer bears a higher quantity of acrylic acid moieties, the peak current in the presence of the BCP exceeds the peak current in the absence of the BCP under basic conditions. This is likely a consequence of preconcentration due to electrostatic attraction, and may further result from channel widening due to the micelle contraction caused by electrostatic repulsion between the pore wall and micelles bearing more negative charges.

It is clear from these results that the polymer structure, specifically the hydrophobic to hydrophilic ratio, can significantly influence and even enhance the ionic permselectivity of mesoporous silica materials due to wetting, electrostatics, and the structure of the resulting films. Further to these results, we present how these assemblies change on incremental changes in pH (Figure 4) and their reversibility (Figure 5). The corresponding CV traces to Figure 4 are given in Figure S6. In Figure S6, we can clearly see that the acrylic acid content influences the pH at which this preconcentration behaviour becomes apparent; for (A) and (C), i.e., at a lower acrylic acid content, preconcentration is only observed under extremely basic conditions of 9–10. Whilst in the presence of higher amounts of acrylic acid units in (B), preconcentration behaviour is observed from ~8, but to a lower extent.

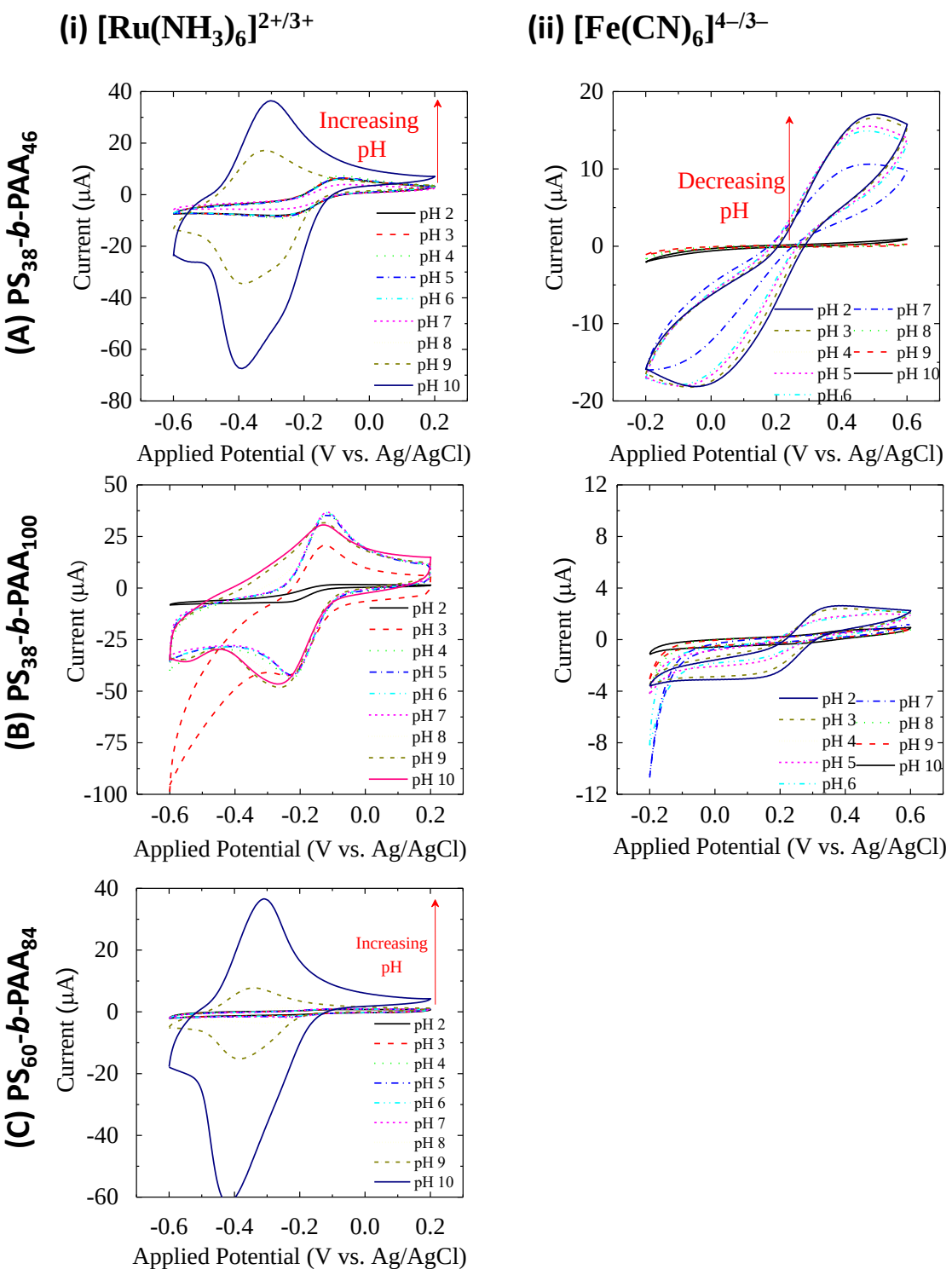

Figure S6 pH-dependent CV traces of mesoporous silica films containing (A) PS_{38}-*b*-PAA_{46}, (B) PS_{38}-*b*-PAA_{100}, and (C) PS_{60}-*b*-PAA_{84}. The CV traces were recorded at a scan rate of 100 mV s^{-1} in a 100 mM KCl electrolyte containing (i) $[Ru(NH_3)_6]^{2+/3+}$ or (ii) $[Fe(CN)_6]^{4-/3-}$ probe molecules at a concentration of 1 mM.

Template Retention under Typical Extraction Conditions

The prepared mesoporous films largely maintain their ionic permselectivity behaviour after being submitted to a harsh acidic ethanol treatment for 3 days as shown in Figure S7. Changes observed before and after treatment including a reduction in the peak current for positive species under basic conditions suggest some loss of the polymer template either through diffusion or degradation; however, the addition of a subsequent layer using a sacrificial template such as F127 will afford step-gradient films for localised polymer functionalisation and provide additional protection against the extraction of the responsive polymer template. This will facilitate superior control over ionic permselectivity for application in lab-on-chip devices. In addition, FTIR spectroscopy before and after solvent extraction suggests the polymer does not degrade (Figure 3).

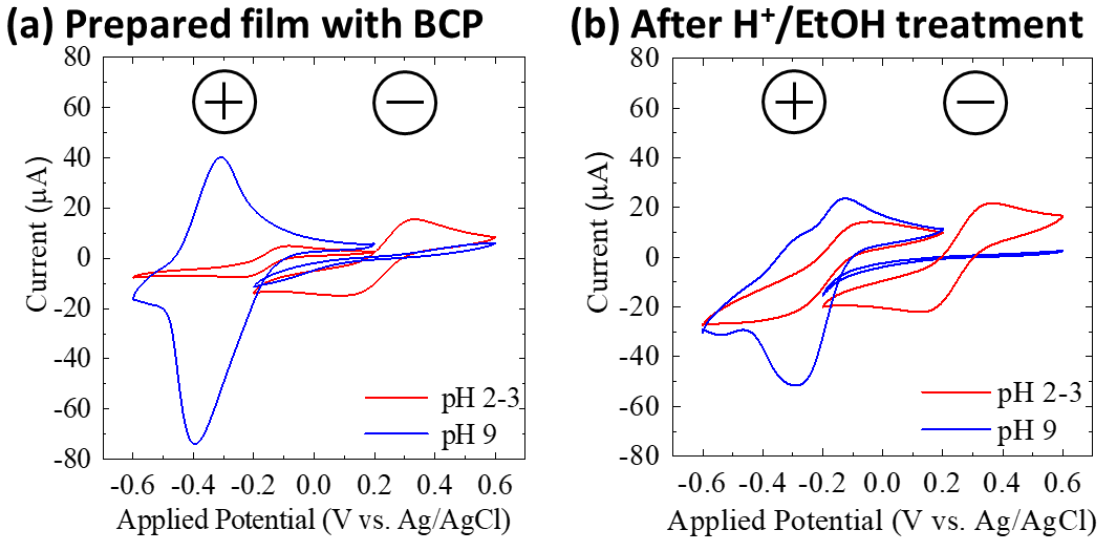

Figure S7 The permselectivity behaviour of the prepared mesoporous silica films structured using PS_{38}-*b*-PAA_{100} as the template block copolymer (a) are largely maintained after being exposed to a H^+/EtOH extraction for 3 days (b). The CV traces were recorded at a scan rate of 100 mV s^{-1} in 100 mM KCl with either $[Fe(CN)_6]^{4-/3-}$ or $[Ru(NH_3)_6]^{2+/3+}$ at a concentration of 1 mM. The reference ITO CV traces varied between approximately 40 and –40 μA, and have been omitted out for simplicity.

Double Layer Mesoporous Silica Films where a Functional Polymer is Entrapped and Confined to a Single Layer

The pH-responsive mesoporous films described above containing an entrapped amphiphilic block copolymer were then coated by a subsequent layer of either silica or aminosilica using F127 as template. The F127 template was then selectively removed from the top layer by solvent extraction. The retention of the functional block copolymer is evident by IR measurements that show bands characteristic of styrene and acrylic acid (Figure S8) of the exposed bottom layer (Figure S9(e)). The presence of the block copolymer template is further confirmed by ellipsometry measurements: A refractive index of ~1.5 for the bottom layer compared to mesoporous silica of ~1.3 is conducive to the presence of high refractive index materials such as PS and PAA (Table S3). These results indicate the successful preparation of step-gradient films where the functional block copolymer is localised in the bottom layer.

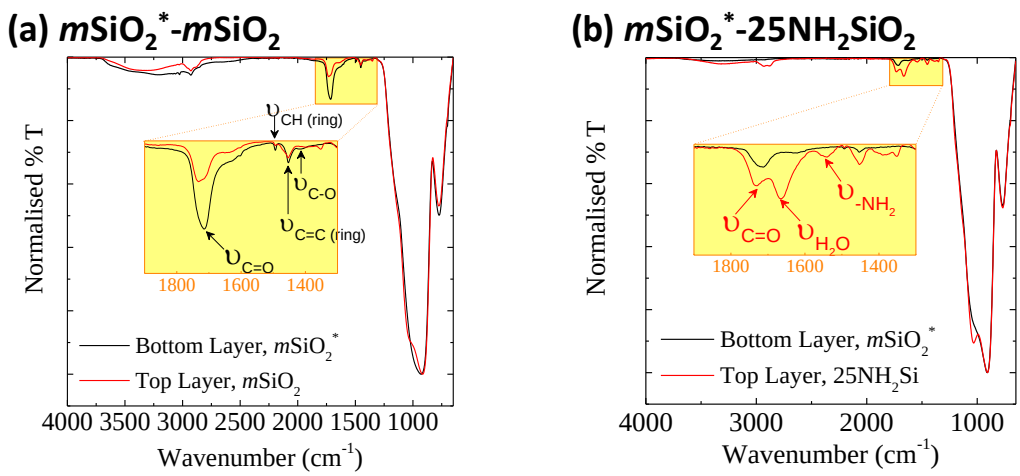

Figure S8 ATR spectra of the bottom and top layer of the prepared step-gradient films with a functional bottom layer with entrapped PS_{38}-*b*-PAA_{100} and either a second mesoporous silica layer (a) or aminosilica layer (b) after solvent extraction in acidic ethanol for 3 days. (*) indicates the functional BCP is present within the material.

Table S3 Average film thickness, refractive index, porosity, and static contact angle of step-gradient films prepared using PS_{38}-*b*-PAA_{100} to template and functionalise the bottom mesoporous silica layer, followed by either a mesoporous silica (Entry 1) or aminosilica (Entry 2, 25 mol% APTMS relative to TEOS) layer templated using F127. The F127 template was removed by a H^+/EtOH extraction for 3 days.

Entry		Material	Template	d_{ave} (nm)[a]	n_{ave}[a]	V_{pore} (%)[b]
	(i)	***m*SiO$_2$***	PS_{38}-*b*-PAA_{100}	133 ± 2	1.47 ± 0.02	---
A	(ii)	***m*SiO$_2$*–*m*SiO$_2$**	F127	374 ± 4	1.34 ± 0.03	30 ± 1
	(iii)	**–*m*SiO$_2$**	F127	176 ± 8	1.28 ± 0.01	38 ± 1
	(i)	***m*SiO$_2$***	PS_{38}-*b*-PAA_{100}	140 ± 4	1.51 ± 0.00	---
B	(ii)	***m*SiO$_2$*–25NH$_2$Si**	F127	413 ± 7	1.31 ± 0.02	32 ± 4
	(iii)	**–25NH$_2$Si**	F127	230 ± 5	1.35 ± 0.00	22 ± 1

*Entries (i) and (iii) correspond to single layer mesoporous silica templated with PS_{38}-*b*-PAA_{100} and Pluronic® F127 after selectively extracting the F127 from the top layer in a 0.01 M HCl ethanolic solution, respectively. Entry (ii) corresponds to a double layer film where the first mesoporous silica layer was templated by PS_{38}-*b*-PAA_{100}, and the second layer was either (A) mesoporous silica or (B) aminosilica (25 mol% APTMS relative to TEOS) templated by F127.
[a]The average diameter, d_{ave}, and refractive index, n_{ave}, were determined by 3 measurements along the film by ellipsometry at a r.H. 15 % at ambient temperature.
[b]The 2-layer system was fitted with a 1-layer model, and the volume porosity was calculated according to the Brüggemann effective medium approximation from the fitted refractive index; this model does not take into account the first layer containing the functional BCP.

The electrochemical properties of these step-gradient films was then assessed via cyclic voltammetry, and the results are shown in Figure 7 and Figure S9 for the mesoporous silica and aminosilica layers, respectively. The mesoporous silica allows positive species to travel freely when the silica channels are highly negatively charged (basic conditions), and gates negative charges irrespective of pH (Figure 7(b), Figure S9(c)). The aminosilica remains relatively closed to both positive and negative charges irrespective of pH (Figure S9(b) and Figure S8(c)).

Due to the poor ionic permselectivity of the double layer films prepared, all organic functions (residual template and amino groups) were removed by an additional thermal treatment to ensure the second sol did not infiltrate the first layer during dip-coating, to hinder the flow of ions through the film. The thermal treatment involved heating the films to 60 °C in 10 min for 1 h before increasing to 100 °C in 10 min for 1 h, and then finally increasing the temperature to 350 °C for 2 h at a rate of 1 °C/min. The results are shown in Figure S9(d). The high permselectivity observed after the removal of the amino functions suggests that the complete exclusion results from electrostatics, and not because of blocked pores since the pores are indeed accessible. A lower amine content may prove more useful here.

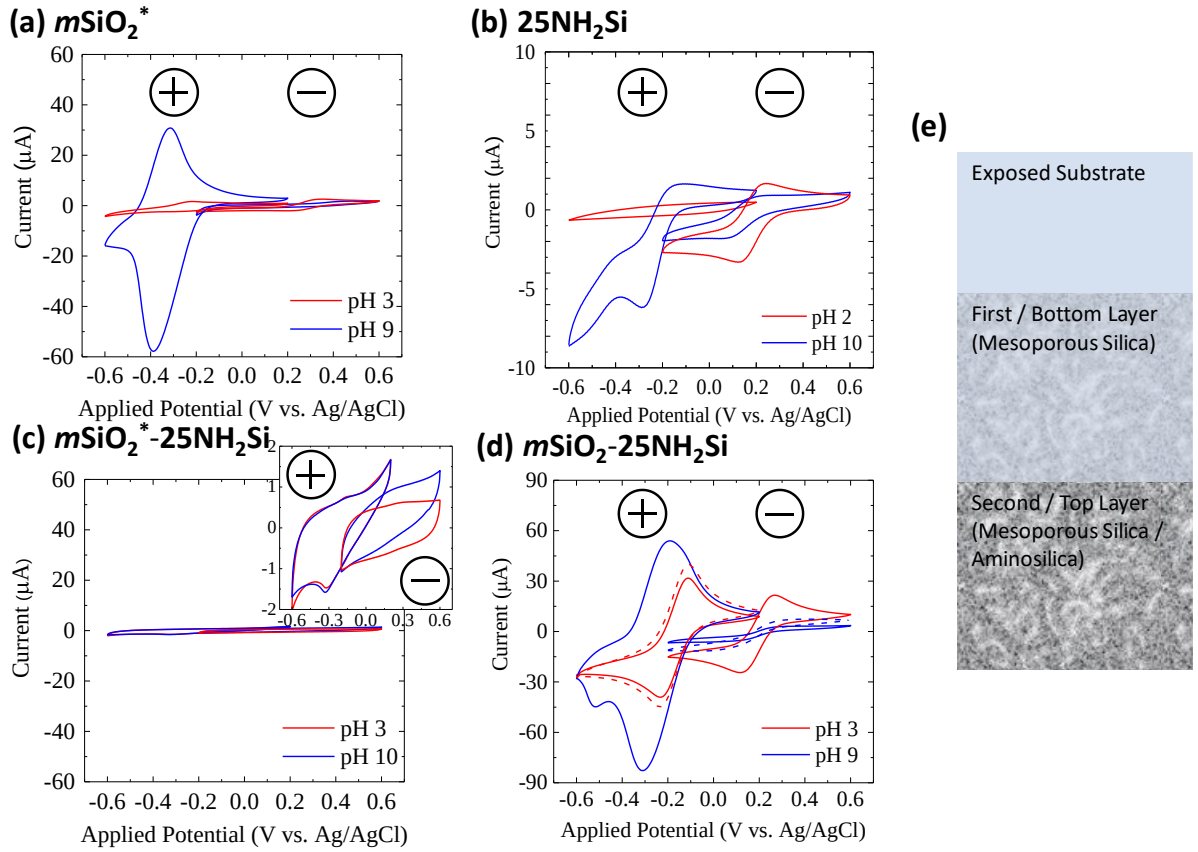

Figure S9 Cyclic voltammograms showing the electrochemical properties of single layer (a) mesoporous silica containing PS_{38}-*b*-PAA_{100} and (b) aminosilica containing 25 mol% APTMS relative to TEOS templated by F127. Since the F127 template is removed selectively by extraction in acidic ethanol for 3 days, double layers could be prepared, and the electrochemical properties (c) before and (d) after an additional calcination at 350 °C to remove all organic material including the entrapped BCP are shown. The CV traces were recorded at a scan rate of 100 mV s^{-1} in a 100 mM KCl electrolyte containing $[Fe(CN)_6]^{4-/3-}$ and $[Ru(NH_3)_6]^{2+/3+}$ at a concentration of 1 mM. The films were incubated in 0.1 M KCl for 30 min prior to recording CV. The (*) indicates the functional BCP is present within the material. In all cases, F127 has been removed. (e) depicts the double layer films prepared by successive dip-coating, with the second film only partially coating the bottom layer, and ideally the pores are perpendicular to the substrate.

Tortuosity of Single Layer Films under Filled and Empty Conditions

The CV traces with varying scan rate was examined to assess the tortuosity of the films before and after removing the functional templates. The CV traces with and without the functional template with varying scan rates are shown in Figure S10 and Figure S11, respectively.

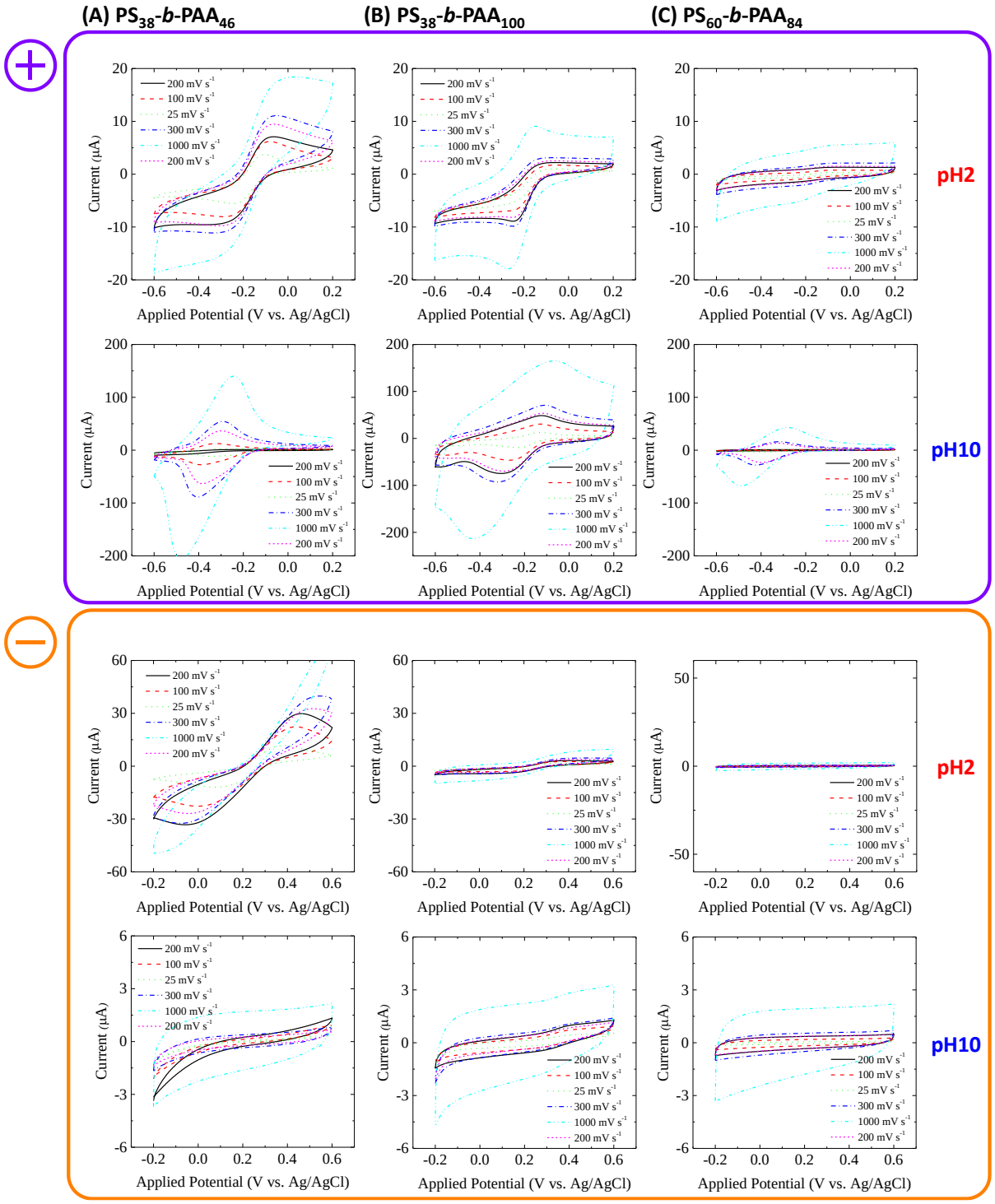

Figure S10 Variation of CV traces of single layer mesoporous silica films with scan rate containing (A) PS_{38}-*b*-PAA_{46}, (B) PS_{38}-*b*-PAA_{100}, and (C) PS_{60}-*b*-PAA_{84}. The CV traces were recorded in a 100 mM KCl electrolyte containing $[Fe(CN)_6]^{4-/3-}$ and $[Ru(NH_3)_6]^{2+/3+}$ at a concentration of 1 mM.

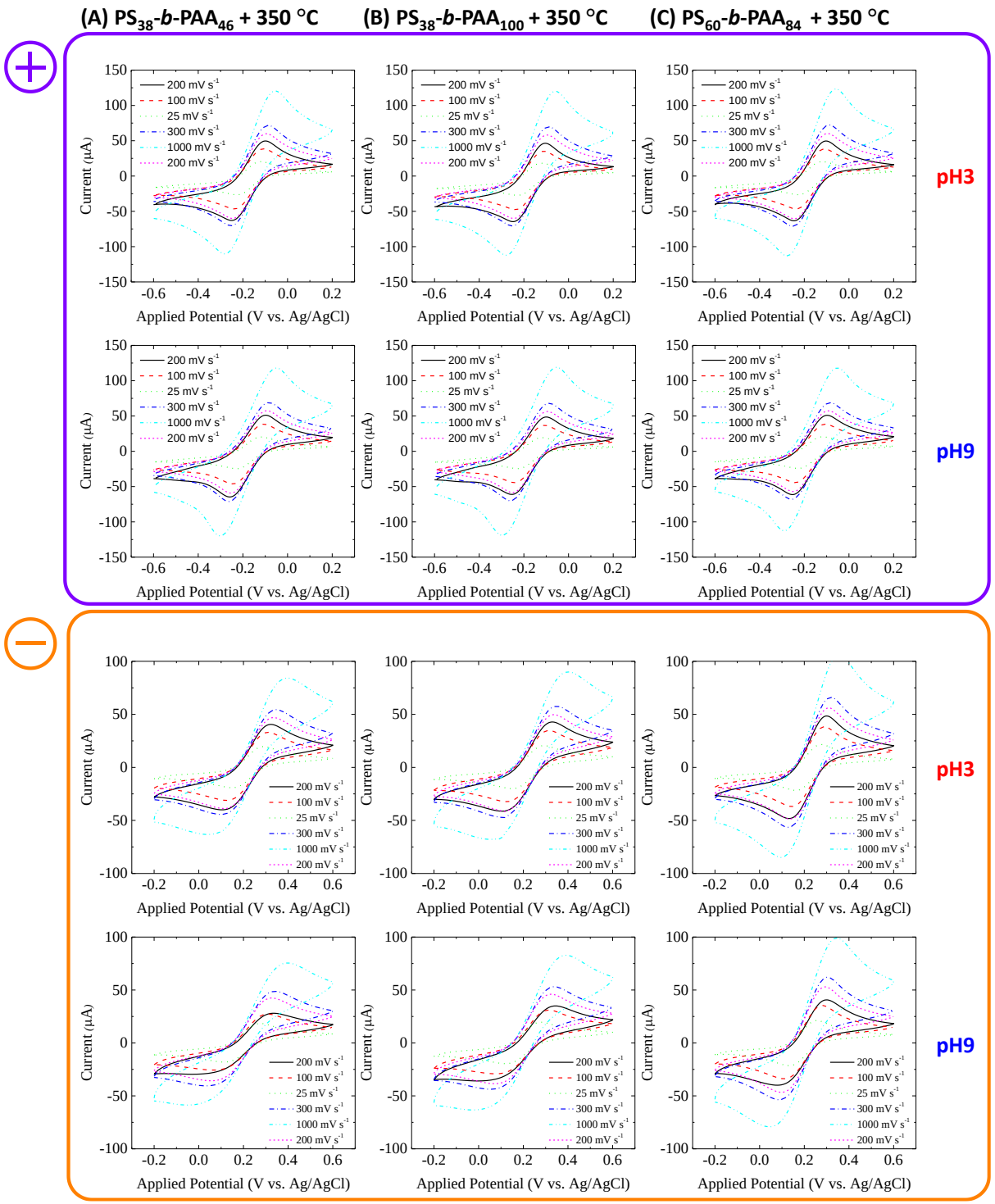

Figure S11 Variation of CV traces of single layer mesoporous silica films with scan rate after removal of the BCP templates at 350 °C. The films above were templated using (A) PS_{38}-*b*-PAA_{46}, (B) PS_{38}-*b*-PAA_{100}, and (C) PS_{60}-*b*-PAA_{84}. The CV traces were recorded in a 100 mM KCl electrolyte containing $[Fe(CN)_6]^{4-/3-}$ and $[Ru(NH_3)_6]^{2+/3+}$ at a concentration of 1 mM.

The variation in peak current with $\upsilon^{1/2}$ was then used to determine the tortuosity of the prepared films in the presence and absence of the functional block copolymer in accordance to a report by Soler-Illia and co-workers published in 2006.[8] The results are summarised in Figure S12 and Table S4. The tortuosity factor is a measure of the pore architecture and level of connectivity. Due to possible pore blocking, reduced wetting, and higher charge density within the polymer-containing pores, a significant reduction in diffusion of charged probe molecules is observed compared to ITO (Figure S12(a)) regardless of the probe or pH. This is in agreement with previous studies where bulky and/or hydrophobic substituents were anchored onto the pore wall.[8] Upon removal of the template by an additional thermal treatment at 350 °C, the tortuosity and/or diffusion is significantly higher (Figure S12(b)), and even shows higher effective diffusion of positive probe molecules as a consequence of pre-concentration within the pores compared to the bare ITO substrate.[8] The variation before and after the thermal treatment further supports the presence of organic material, i.e., the BCP templates, within the pores.

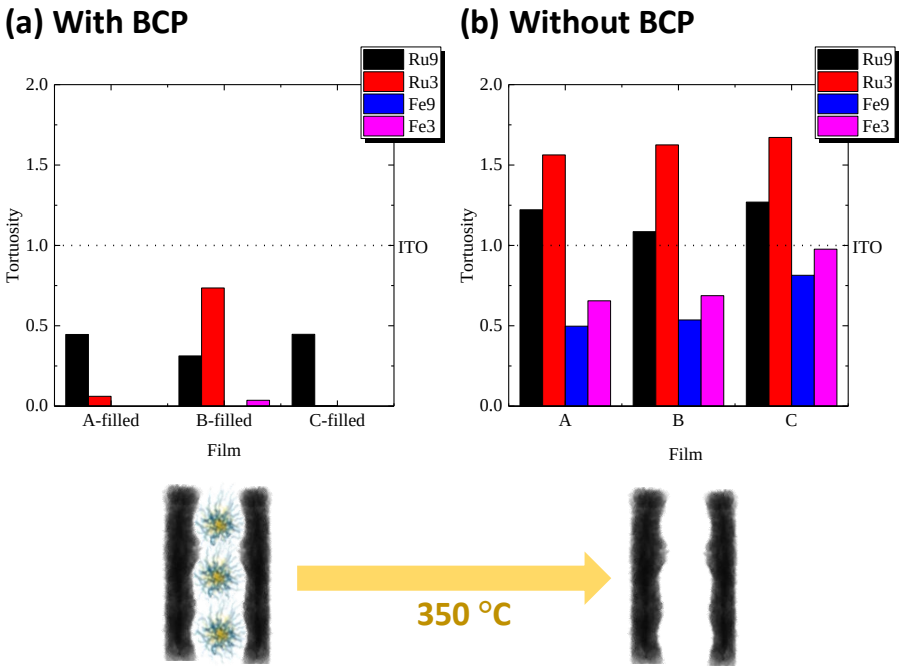

Figure S12 Tortuosity of the prepared single layer mesoporous films before and after an additional thermal treatment at 350 °C to remove the functional BCP template.

Table S4 Summary of the tortuosity values of single layer mesoporous silica films before and after template removal compared to the substrate, ITO, using various probes and pH values.

		Ru9	Ru3	Fe9	Fe3
Substrate	ITO	1.00	1.00	1.00	1.00
Filled	Film A	0.45	0.06	0.00	*
	Film B	0.31	0.74	0.00	0.04
	Film C	0.45	0.00	0.00	0.00
Empty	Film A	1.22	1.56	0.50	0.66
	Film B	1.09	1.63	0.54	0.69
	Film C	1.27	1.67	0.81	0.98

*Could not be determined due to signal broadening.

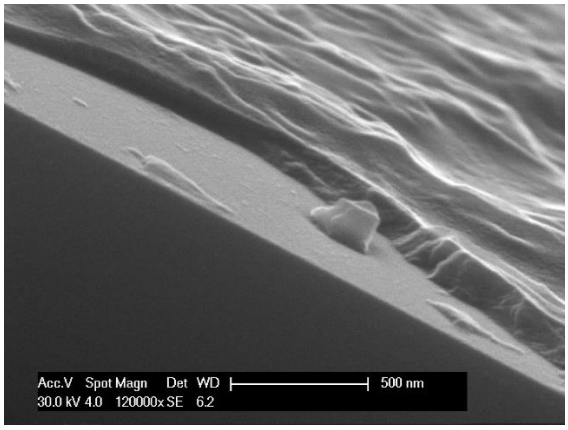

Figure S*13* SEM micrograph (cross section) of a mesoporous silica film templated with PS38-*b*-PAA46 corresponding to Figure 2a.

Characterisation of the mesoporous surface structure using GISAXS

GISAXS measurements were performed on two mesoporous silica films templated with PS_{38}-b-PAA_{46} and PS_{38}-*b*-PAA_{100} (compare Figure 2). The silica wafers were placed in a point-focussed beam and illuminated under an incident angle of α_i = 0.2° (roughly $0.85\alpha_{c,silica}$). The scattered intensity was measured in a 2D detector with a dimension of 775 x 385 px^2. In the images in Figure S14, pixels have already been converted into q-space with the definition of $q_{||}$ and q_z as depicted in the analytical method section. A beamstop was placed around $|q_{||}| < 0.23$ nm^{-1} and $q_z < 1$ nm^{-1} which cuts out the specularly reflected signal.

Figure S14 clearly shows strong scattering from surface structure of the films. The two long streaks of high intensity at approximately constant $q_z \approx 0.4 nm^{-1}$ are attributed to the Yoneda peak, an anomalous scattering phenomena occurring at the critical angle. The appearance of the Yoneda peak itself is another indicator for strong scattering from structures within the surface plane. To quantitatively investigate the scattering within the surface plane, intensity is extracted along the red box in direction of $q_{||}$ as indicated in both images. Resulting scattering profiles are shown in Figure S15.

For both samples, the scattered intensity at small $q_{||}$ is cut off due to the beamstop placed in front of the detector. For larger $q_{||}$, intensity decays before approaching the background level of 0.2 around $q_{||} = 1 nm^{-1}$. The form factor of oriented cylinders with a polydisperse diameter is fitted to the data in the range of $0.5 nm^{-1} \leq q_{||} \leq 1 nm^{-1}$. We get a nice agreement between experimental data and fitted form factor. The form factor leads to very similar pore diameters for Sample A, PS_{38}-*b*-PAA_{46}, and B, PS_{38}-*b*-PAA_{100}: d_A=(6.8 ± 1.7) nm and d_A=(7.3 ± 1.8) nm. Moreover, there is additional intensity at low $q_{||} \approx 0.3$-$0.4 nm^{-1}$, which appears to be more distinct for PS_{38}-*b*-PAA_{46}. It may be due to the appearance of a structure peak.

To compare the pore diameter from reciprocal and real space, we have attached the 2D fourier transform of the TEM images A and B of Figure 2 from the main manuscript as an inset in the figure. The structure revealed by these images agree with the sizes obtained in GiSAXS. We note that image 2B indicates an oriented lamellar structure, which leads to sharp points lying on a line in q-space. However, our scattering results averages over larger areas in which different orientations compare as seen at the lower resolution images of the SEM.

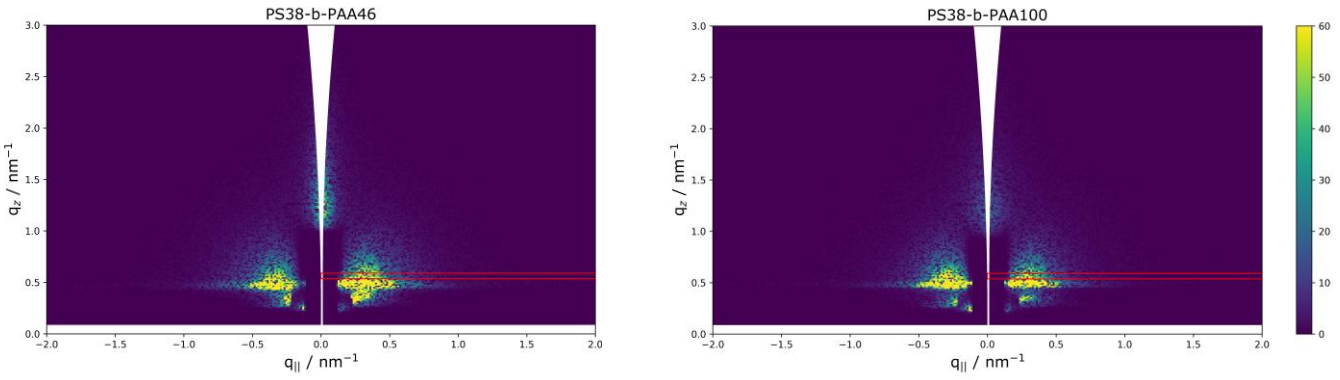

Figure S*14* GISAXS detector image with pixels converted into q-space ($q_{||}$ and q_z). The scale bar illustrates the intensity in arbitrary units

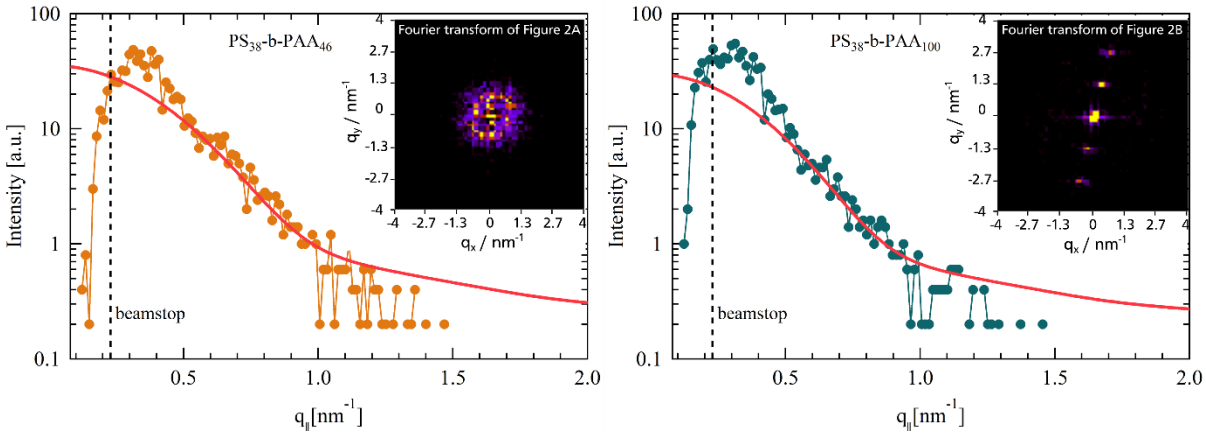

Figure S15 *In-plane scattering as Intensity vs $q_{//}$ extracted from the red box in Figure S14.The insets are respectively the 2D fourier transforms of the real space TEM images from Figure 2 of the main manuscript.*

References

1 C. Boissiere, D. Grosso, S. Lepoutre, L. Nicole, A. B. Bruneau and C. Sanchez, *Langmuir*, 2005, **21**, 12362.

2 A. Brunsen, A. Calvo, F. J. Williams, G. J. A. A. Soler-Illia and O. Azzaroni, *Langmuir*, 2011, **27**, 4328.

3 J. Tom, B. Hornby, A. West, S. Harrisson and S. Perrier, *Polym. Chem.*, 2010, **1**, 420.

4 W. Liu, J. Mao, Y. Xue, Z. Zhao, H. Zhang and X. Ji, *Langmuir*, 2016, **32**, 7596.

5 M. Wiśniewska, T. Urban, E. Grządka, V. I. Zarko and V. M. Gun'ko, *Colloid and Polymer Science*, 2014, **292**, 699.

6 M. Tagliazucchi and I. Szleifer, *Materials Today*, 2015, **18**, 131.

7 S. Alberti, P. Y. Steinberg, G. Giménez, H. Amenitsch, G. Ybarra, O. Azzaroni, P. C. Angelomé and G. J. A. A. Soler-Illia, *Langmuir*, 2019, **35**, 6279.

8 E. H. Otal, P. C. Angelomé, S. A. Bilmes and G. J. A. A. Soler-Illia, *Adv. Mater.*, 2006, **18**, 934.

Figure S15 2erngernt